DOI: https://doi.org/10.30898/1684-1719.2026.9.6

The effect of clay and organic matter content on the relaxation time distribution in mineral-organic soils

Yu.I. Lukin, A.Yu. Karavayskiy

Kirensky Institute of Physics
– Federal Research Center "Krasnoyarsk Science Center of the Siberian Branch of the Russian Academy of Sciences"
Russia, Krasnoyarsk

The paper was received August 8, 2026.

Abstract. The spectra of complex dielectric permittivity of three soils with different granulometric composition and different organic matter content were measured in the frequency range from 15 MHz to 15 GHz and in the moisture range from dry state to the minimum water-holding capacity at a temperature of 25°C. From the complex dielectric permittivity spectra obtained the relaxation time distribution functions were retrieved. Analysis of the relaxation time distribution functions revealed up to nine relaxation processes for all specimens, grouped by characteristic times: 6–50 ps, 20–120 ps, 800–20·103 ps and from 104 to greater than 105 ps. Comparison with literature data allowed attributing the slowest group to the Maxwell- Wagner relaxation, the second and third groups to bound water relaxations, while the first group includes contributions from both unbound and bound water. It was found that an increase in moisture leads to an increase in relaxation times and a broadening of their distribution, most noticeable in the third group. A qualitative similarity in the effect of clay and organic matter content on relaxation parameters was demonstrated, while the times of the extreme high-frequency and low-frequency processes remain practically

independent of soil composition. Non-monotonic changes in the times of intermediate relaxations with varying organo-mineral composition were noted.

Key words: dielectric relaxation, relaxation time distribution function, complex dielectric permittivity, moist soil, organomineral soil, Maxwell-Wagner polarization, bound water.

Financing: The work was carried out within the framework of the scientific topic of the State Assignment of the Kirensky Institute of Physics of the Siberian Branch of the Russian Academy of Sciences.

Corresponding author: Karavayskiy Andrey Yurievich, rsdak@ksc.krasn.ru

Introduction

The development of radio-physical remote sensing methods of the Earth is one of the key directions in modern geophysics, climatology, and environmental monitoring. Satellite radar and radiometric systems (such as SMOS, SMAP, Sentinel-1) enable global, operational, and all-weather monitoring of soil moisture, freeze-thaw processes in soils, and the state of the vegetation layer. The physical basis of these methods relies on the existence of a fundamental relationship between the recorded characteristics of natural thermal emission (brightness temperature) or backscattering (specific effective scattering coefficient) and the electrodynamic parameters of the natural object.

The main electrodynamic parameter determining the processes of absorption, refraction, and scattering of electromagnetic waves in soil is the dielectric permittivity (DP). For media with absorption of electromagnetic (EM) waves, which also include wet soils, this quantity is complex dielectric permittivity (CDP). In addition, wet soils exhibit frequency dispersion of the CDP. Accurate interpretation of aerospace monitoring data is impossible without constructing adequate broadband dielectric models that link the physicochemical properties of soils to their CDP [1]. Understanding the nature and patterns of formation of the frequency spectra of soil CDP across the entire radio frequency range is a crucial fundamental and applied

problem. Its solution allows minimizing errors in retrieving natural soil characteristics, such as moisture or temperature, from ERS data [2].

Soil is a heterogeneous, multicomponent, and porous disperse system consisting of a solid mineral matrix, organic matter, soil solution (water), and air. The frequency dependence of the soil CDP spectrum is influenced by a set of interrelated factors. First and foremost is moisture. In the frequency range of radio-physical remote sensing, the CDP of water significantly exceeds the values of this quantity for other soil components. Therefore, moisture is the dominant factor determining the CDP value of the mixture [1; 3]. Water in soils can be categorized by the degree of bonding with solid particles: strongly bound, loosely bound, and unbound (free) water. It is known that the CDP of different categories of soil water differs. The mineral composition and specific surface area of solid particles (especially clay and organic fractions) determine the ratio between different categories of soil moisture. A high clay content increases the maximum bound water content threshold, strongly altering the shape of the CDP spectrum [4]. The packing density of soil aggregates affects the volume fraction of mineral and organic components and pore geometry, and consequently the soil CDP value [5]. Temperature changes alter the viscosity of soil water, dipole relaxation times, and ionic mobility, which is reflected in the temperature coefficient of CDP, especially during the freeze-thaw transition [6]. The salinity of the soil solution significantly affects the imaginary part of CDP in the frequency range up to 1 GHz. This is because the concentration of free ions determines the ionic conductivity, which makes a dominant contribution to the imaginary part of CDP at low frequencies [7].

The CDP spectrum has a complicated shape due to the influence of multiple dielectric relaxations, with the influence ranges of these relaxations overlapping. First, this is the relaxation of unbound water in the range from 10 GHz to 30 GHz. This relaxation is determined by the orientational polarization of bulk water molecules via the Debye mechanism. The EM loss maximum at room temperature occurs at a frequency of about 17 − 19 GHz [8]. The range from 100 MHz to 8 GHz corresponds to the relaxation of bound water. Since bound water molecules are under the influence of strong sorption fields on the surface of clay minerals or organic particles and are

restricted in their mobility, their relaxation time increases by 1-2 orders of magnitude compared to which of unbound water. The relaxation frequency of bound water is distributed over a wide range and decreases as the monolayer is approached, reaching values of approximately 100 MHz for strongly bound (hygroscopic) moisture [9]. In the range of 10 kHz − 100 MHz, Maxwell-Wagner (MW) interfacial polarization occurs. This relaxation is due to the accumulation of free charges and ions at phase boundaries with different DPs and conductivities (the “mineral – solution”, “organic – solution”, and pore walls boundaries). The process is characterized by long relaxation times and contributes enormously to the CDP values at the operating frequencies of FDR and TDR instruments [10]. The range below 10 kHz corresponds to the region dominated by relaxation associated with ion diffusion in the electrical double layer (EDL) around soil particles.

Traditional approaches based on Debye and Cole-Cole models with a fixed set of relaxators [11] encounter difficulties in modeling soil media due to strong spatial and structural heterogeneity. In heterogeneous matrices, the relaxation time spectrum is broadened. The most rigorous and physically sound method for describing such continuous dispersion is the introduction of a continuous relaxation time distribution function (RTDF) – $g(\tau)$ [12].

The relationship between the measured CDP $\varepsilon^*(\omega)$ and the RTDF is expressed by the Fredholm integral equation of the first kind:

$$\varepsilon^* = \varepsilon_\infty + (\varepsilon_0 - \varepsilon_\infty)\int_{-\infty}^{\infty} \frac{G(\tau)d(\lg\tau)}{1+i\omega\tau} + i\frac{\sigma}{\omega\varepsilon_r}, \quad (1)$$

where $\varepsilon^* = \varepsilon' + i\varepsilon''$ is the soil CDP; ε' and ε'' are its real and imaginary parts, respectively; $i = \sqrt{-1}$; ε_∞ and ε_0 are the high-frequency and low-frequency limits of the DP (HFLDP and LFLDP); τ is the relaxation time; $G(\tau)$ is the RTDF; $\omega = 2\pi f$ is the angular frequency (f is the EM field frequency); σ is the sample conductivity; $\varepsilon_r = 8.854 \cdot 10^{-12}$ F/m is the permittivity of free space. Formula (1) can be considered as an equation for the unknown quantities $G(\tau)$, ε_∞, ε_0, and σ.

Determining the function G(τ) from experimental CDP spectra $\varepsilon^*(\omega)$ is an ill-posed inverse problem. Its numerical solution requires the application of specialized mathematical algorithms, such as the Tikhonov regularization method [13].

Historically, the apparatus of RTDF was actively developed in the physics of polymers, ferroelectrics, glasses, and complex organic systems for separating overlapping polarization mechanisms [14]. In recent decades, the concept of relaxation time distribution has made a breakthrough in the field of electrochemical impedance spectroscopy for diagnostics of fuel cells, supercapacitors, and lithium-ion batteries [15]. Using this method, researchers successfully separate charge transfer, diffusion, and interfacial resistance processes.

In geophysics and soil science, the application of the continuous RTDF basis has long been constrained by the complexity of numerical inversion and a shortage of broadband experimental data. However, in recent works [16, 17], it was clearly demonstrated that retrieving $G(\tau)$ from experimental soil spectra in the range from 15 MHz to 15 GHz allows analyzing the influence of individual dielectric relaxations in soils, as well as isolating the contribution of MW interfacial polarization and direct current (DC) conductivity, caused by the movement of free ions in the soil solution, from bound and unbound water relaxations without introducing artificial fitting empirical parameters or assumptions within dielectric models.

Previously, in the work [16], the RTDF of a forest organo-mineral soil were investigated as a function of temperature in both frozen and thawed states. In the present work, the results of a study on the effect of soil granulometric composition on the RTDF using three organo-mineral soils as examples are provided.

1. Methods and Materials

The objects of study were three organo-mineral soils with different clay and organic matter contents. The granulometric composition of the soils and the organic matter content are given in Table 1.

Table 1. Granulometric composition and organic content of soils.

Soil	Clay (USDA), <0.002 mm	Silt, 0.002-0.05 mm	Sand, 0.05-2 mm	Organic matter
Specimen 1	10.65	47.95	41.4	0.9
Specimen 2	23.32	66.18	10.5	11.1
Specimen 3	31.65	63.25	5.1	14.6

Measurements of soil CDP spectra were carried out at a temperature of 25 °C and in the moisture range from dry state to the minimum water-holding capacity. Before measurements, samples with a uniform moisture distribution from minimum to maximum were prepared. The samples were kept in sealed weighing bottles for two weeks to allow the water to be uniformly distributed throughout the sample volume. Then, measurements of the S_{12}-parameters of the scattering matrix spectra were carried out in the EM field frequency range from 15 MHz to 15 GHz. Using the method described in [18], the frequency spectra of the CDP parameters for each sample were calculated from the measured S_{12}-parameter spectra.

For the RTDF calculation, the method described in [17] was used. The RTDF reconstruction was carried out by numerically solving equation (1).

Since the experimental CDP data of soil samples are a discrete dataset in which each frequency f_i from n measurements in a given frequency range corresponds to a measured i-th value of the real and imaginary parts of the CDP, one can also define an arbitrary discrete grid for the RTDF argument τ consisting of m values and seek the value of the function $G(\tau)$ for each τ_j-th argument. Then equation (1) reduces to the following system of linear equations:

$$\begin{cases} \varepsilon'_j = \varepsilon_\infty + \sum_{i=1}^{m} \dfrac{\Delta\varepsilon_i}{1+\left(\omega_j\tau_i\right)^2}, \\ \varepsilon''_j = \sum_{i=1}^{m} \dfrac{\Delta\varepsilon_i\left(\omega_j\tau_i\right)}{1+\left(\omega_j\tau_i\right)^2} + \dfrac{\sigma}{\varepsilon_r\omega_j}. \end{cases} \quad (2)$$

The solution of equation (2) was carried out using the Tikhonov regularization method and the *nnls* function from the *scipy.optimize* package of the *Python* programming language for minimization of the following functional:

$$\Phi = \mathbf{Y} - \mathbf{B}\mathbf{X}^2 + \alpha^2 \mathbf{R}\mathbf{X}^2, \tag{3}$$

where α is the regularization coefficient, **R** is the regularization operator of the following form:

$$\mathbf{R}_{2n\times(m+2)} = \begin{pmatrix} h_\tau^2 & 0 & 0 & 0 & 0 & \cdots & 0 & 0 \\ 0 & h_\tau^2 & 0 & 0 & 0 & \cdots & 0 & 0 \\ 0 & 1 & -2 & 1 & 0 & \cdots & 0 & 0 \\ 0 & 0 & 1 & -2 & 1 & \cdots & 0 & 0 \\ \cdots & \cdots & \cdots & \cdots & \cdots & \cdots & \cdots & \cdots \\ 0 & \cdots & \cdots & 0 & 1 & -2 & 1 & 0 \\ 0 & \cdots & \cdots & \cdots & \cdots & 0 & h_\tau^2 & 0 \\ 0 & \cdots & \cdots & \cdots & \cdots & \cdots & 0 & h_\tau^2 \end{pmatrix},$$

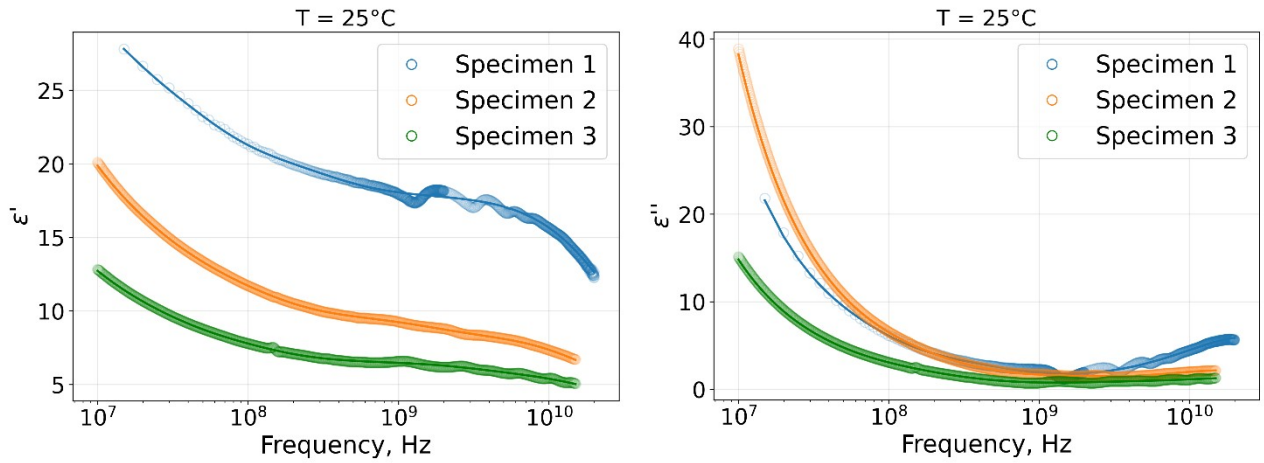
h_τ is the grid step of the τ interval,

$$\mathbf{Y}_{2n} = \begin{pmatrix} \varepsilon_1' \\ \cdots \\ \varepsilon_n' \\ \varepsilon_1'' \\ \cdots \\ \varepsilon_n'' \end{pmatrix}, \quad \mathbf{B}_{2n\times(m+2)} = \begin{pmatrix} 1 & \frac{1}{1+\omega_1\tau_1} & \cdots & \frac{1}{1+\omega_1\tau_m} & 0 \\ \cdots & \cdots & \cdots & \cdots & \cdots \\ 1 & \frac{1}{1+\omega_n\tau_1} & \cdots & \frac{1}{1+\omega_n\tau_m} & 0 \\ 0 & \frac{\omega_1\tau_1}{1+\omega_1\tau_1} & \cdots & \frac{\omega_1\tau_m}{1+\omega_1\tau_m} & 1 \\ \cdots & \cdots & \cdots & \cdots & \cdots \\ 0 & \frac{\omega_n\tau_1}{1+\omega_n\tau_1} & \cdots & \frac{\omega_n\tau_m}{1+\omega_n\tau_m} & 1 \end{pmatrix},$$

$$\mathbf{X}_{m+2} = \begin{pmatrix} \varepsilon_\infty \\ \Delta\varepsilon_1 \\ \cdots \\ \Delta\varepsilon_m \\ \sigma \end{pmatrix}.$$

2. Results and Discussion

Figure 1 shows, as an example, the experimental (symbols) and calculated using the found RTDFs (lines) spectra of the real (a) and imaginary (b) parts of the CDP for three soils at the same moisture content M_g = 0.15 g/g. Good agreement between the model and experiment is confirmed by low values of the normalized root mean square deviation: 0.83% for ε' and 4.25% for ε''. Despite the same moisture content, the ε' values of the soils in the considered frequency range differ systematically: specimen 1 (lowest clay and organic matter content) is characterized by the largest value, while specimen 3 (highest clay and organic matter content) shows the smallest ones. Specimen 2 occupies an intermediate position in terms of ε' value. This is explained by the fact that in soils with a high content of clay fractions and organic matter, the proportion of bound water increases, whose dielectric permittivity is lower than that of unbound water. For the imaginary part of the CDP, more complex behavior is observed. In the low-frequency region (15–300 MHz), the highest ε'' values were observed for specimen 2 (middle clay and organic matter content), while for specimen 3 (maximum clay and organic matter content) they are minimal. In the 1–15 GHz range, the differences smooth out: the ε'' values for specimens 2 and 3 become close, while specimen 1 shows the highest values. The obtained data indicate that in the low-frequency region, DC ionic conductivity, which depends on the composition of the soil solution and the content of bound water, plays a determining role, while in the gigahertz range, dipole relaxation mechanisms make a larger contribution.



a b

Figure 1. Frequency spectra of ε′ (a) and ε″ (б) of soils with moisture M_g = 0.15 g/g. Symbols denote experimental data, lines denote the results of spectrum calculation using the obtained RTDFs.

The value of ε' monotonically decreases with increasing frequency across the entire considered frequency range; however, the rate of decrease is not uniform; in the range from 100 MHz to 6 GHz, the changes are minimal. The value of ε'' has a minimum at frequencies around 1 GHz. Such a CDP spectrum is characteristic of dielectrics with several relaxation processes whose relaxation times differ significantly. This is confirmed by the shape of the relaxation time distribution functions (see Fig. 2), which clearly show from three (in dry samples) to seven (in wet samples) peaks. The widths of the peaks are significantly smaller than the RTDF search range, so one can speak of the proximity of the function to a discrete form. From literature sources [19; 20], it is known that the relaxation time range from 8 to 60 ps corresponds to the orientational relaxation of unbound water. The range of τ from $1.5 \cdot 10^3$ to $2 \cdot 10^5$ ps relates to the Maxwell-Wagner (MW) interfacial relaxation. The intermediate RTDF peaks correspond to bound water relaxations. The multiplicity of RTDF relaxation peaks in this region reflects the heterogeneity of the states of bound water molecules. In the work [16], it was also established that the region of bound and unbound water relaxations overlaps, so it is impossible to distinguish these types of water in the RTDF.

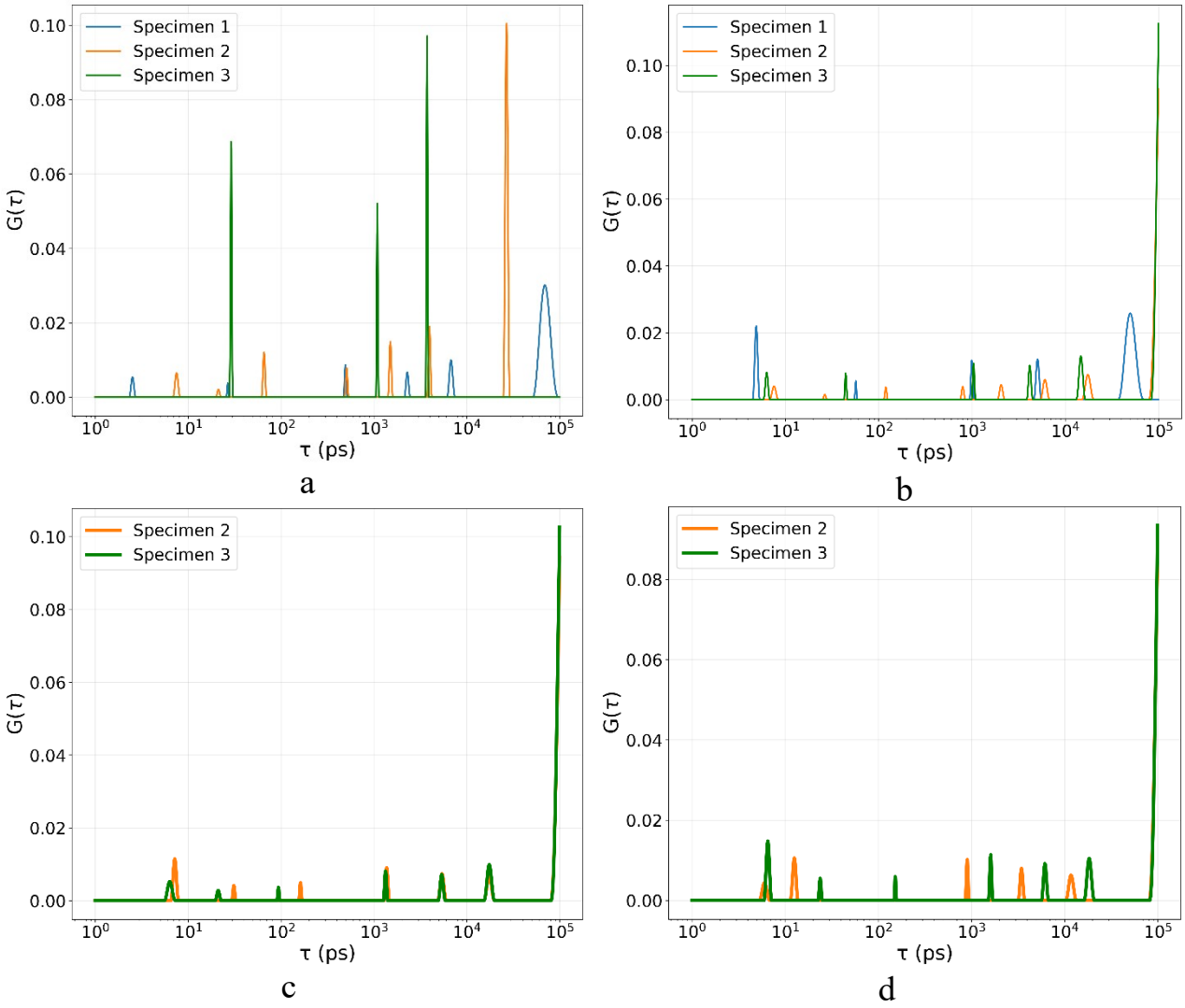
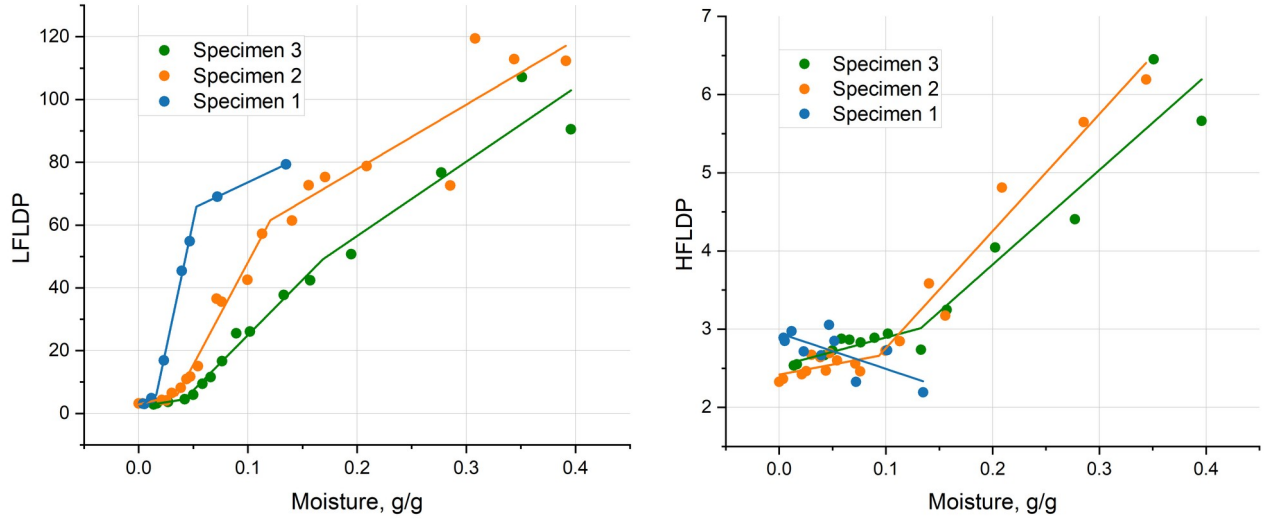


Figure 2. RTDFs of soil samples with moistures of 0.03 g/g (a), 0.10 g/g (b), 0.20 g/g (c) and 0.30 g/g (d).

Analysis of the relaxation processes depending on the composition and moisture of the samples allows identifying some patterns. In the sample with middle clay and organic matter content the low-frequency MW relaxation with τ about $3 \cdot 10^4$ ps dominates. For the soil with the highest sand content, along with the low-frequency relaxation, the relaxation with τ about 50 ps has a significant influence. In specimen 3 with the maximum clay and organic matter content, at a moisture of 0.03 g/g, the RTDF peak with τ about 3000 ps has the largest magnitude, while the low-frequency MW relaxation is absent. With increasing moisture, the Maxwell-Wagner relaxation becomes the dominant relaxation process for all studied specimens.

In addition to the RTDF, the following soil parameters were determined from the CDP spectra: LFLDP, HFLDP, and DC conductivity. Figure 3 shows the obtained

LFLDP and HFLDP of the soils as a function of moisture. These dependences have noticeable breaks delimiting regions with different growth rates of these quantities. In the low moisture region, the LFLDP values have breaks for specimens 1, 2, and 3 at points corresponding to moistures of 0.015, 0.035, and 0.042 g/g. The next break for the studied samples corresponds to moistures of 0.05, 0.12, and 0.17 g/g. The HFLDP for specimen 1 has no breaks; for specimen 2 and 3, only one break is clearly distinguishable near 0.09 and 0.13 g/g, respectively. In works [3; 21] breaks in the moisture dependence of soil CDP are explained by the difference in the CDP of soil water categories: tightly bound, loosely bound, and unbound water. This hypothesis is confirmed by the nature of the moisture dependence of conductivity shown in Fig. 4. The conductivity is close to zero at moistures of 0.07, 0.08, and 0.10 g/g for specimens 1, 2, and 3, respectively; at higher moistures, conductivity growth is observed for all soils. From the literature [22] it is known that bound water has low conductive properties, while the appearance of unbound water provides an increase in electrical conductivity. Thus, the breaks in LFLDP reflect the sequential filling of pore space with various categories of water, while the growth of conductivity begins only when moisture is sufficient for the formation of continuous conductive paths.



a b

Figure 3. LFLDP (a) and HFLDP (b) of soils as a function of moisture.

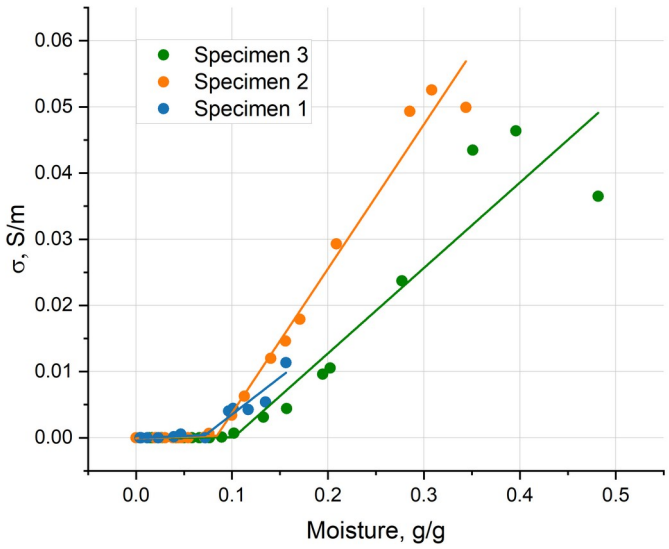


Figure 4. DC conductivity of soils as a function of moisture.

Analysis of soil CDP spectra at the same moisture content (Fig. 1) revealed the influence of granulometric composition on the dielectric response which is due to the different content of bound water. Indeed, with an increase in the proportion of clay particles and organic matter, the specific surface area of the solid phase increases and, consequently, the content of bound water. This is consistent with the position of the breaks in Figs. 3 and 4: the higher the content of clay and organic matter, the higher the moisture at which the appearance of water volumes of another category is observed. For a quantitative assessment of the effect of clay and organic matter content on the dielectric relaxation times of soils, corresponding dependences were constructed in Figs. 5 for specimens at a moisture of 0.15 g/g. As can be seen from the figures, the nature of the dependence on both clay and organic matter content is identical. Their content has practically no effect on the high-frequency relaxation with a time of about 6 ps and on the MW relaxation with a time of about 10^5 ps. The relaxations related to bound water show some dependence. The relaxation times around 700 and 3000 ps decrease with increasing clay and organic matter. The dependences of the relaxation times around 20 and 10^4 ps have a non-monotonic character: in the first case, a minimum is observed; in the second, a weakly expressed maximum at intermediate contents.

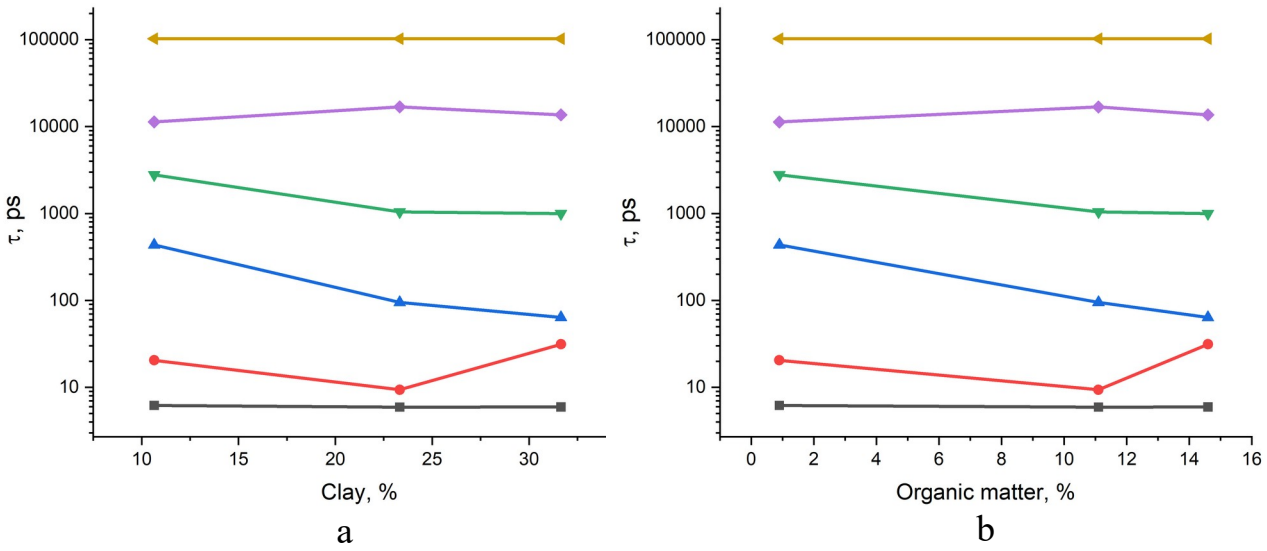


Figure 5. Relaxation times in organo-mineral soils as a function of clay (a) and organic matter (b) content.

To study in detail the effect of moisture on the RTDF of the studied soils, diagrams shown in Figs. 6-7 were constructed, in which the RTDF is shown as a projection of the arguments of moisture and relaxation time. In general, for all soils, a tendency to increase the relaxation time with increasing moisture can be observed, as well as an increase in the number of relaxation peaks. The largest magnitude in the entire studied range is the peak corresponding to the low-frequency MW relaxation with a time of about 10^5 ps. In the samples at low moistures, two or three relaxation processes are identified with times in the ranges of 10−100 ps and 10^3−10^4 ps. The MW relaxation is present in the entire studied moisture range for specimen 2, while in the other samples it is identified at moistures greater than 2%. With a further increase in moisture, a group of high-frequency relaxations with times in the range from 5 to 15 ps appears. For specimens 1 and 2, they appear at moistures greater than 0.02 g/g, for specimen 3 at a moisture of about 0.04 g/g. With increasing moisture, relaxations with times in the range of 10^3 – $5 \cdot 10^4$ ps appear, a significant part of which are formed as a result of the splitting of peaks that appeared at lower moistures. The splitting of the peak is evidenced by the disappearance of the RTDF peak and the appearance of neighboring peaks with close time values; with a further increase in moisture, these peaks diverge, i.e. the time of one increase and the other decrease.

This phenomenon is most clearly observed for specimen 2, where peak splitting occurs at moistures of 0.02 and 0.06 g/g with times of $2 \cdot 10^3$ and $8 \cdot 10^3$ ps respectively.

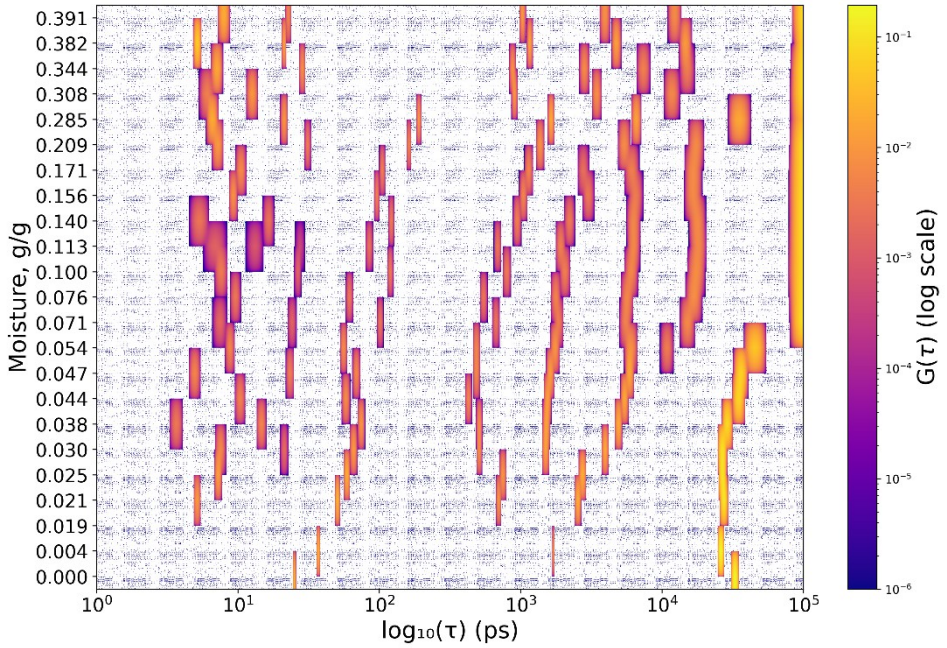


Figure 6. Diagram of RTDF variation of specimen 2 as a function of moisture.

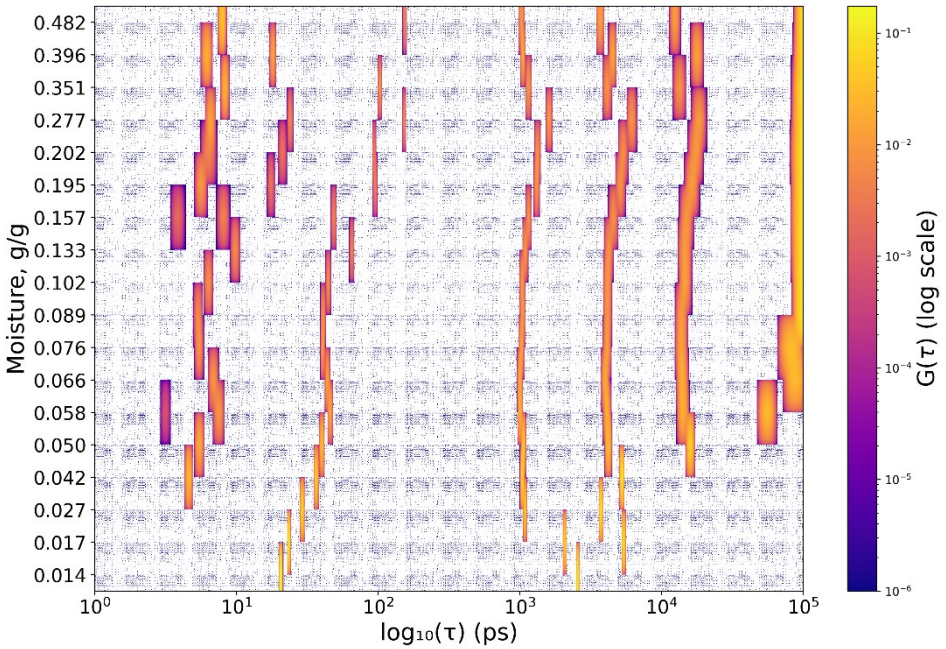


Figure 7. Diagram of RTDF variation of specimen 3 soil as a function of moisture.

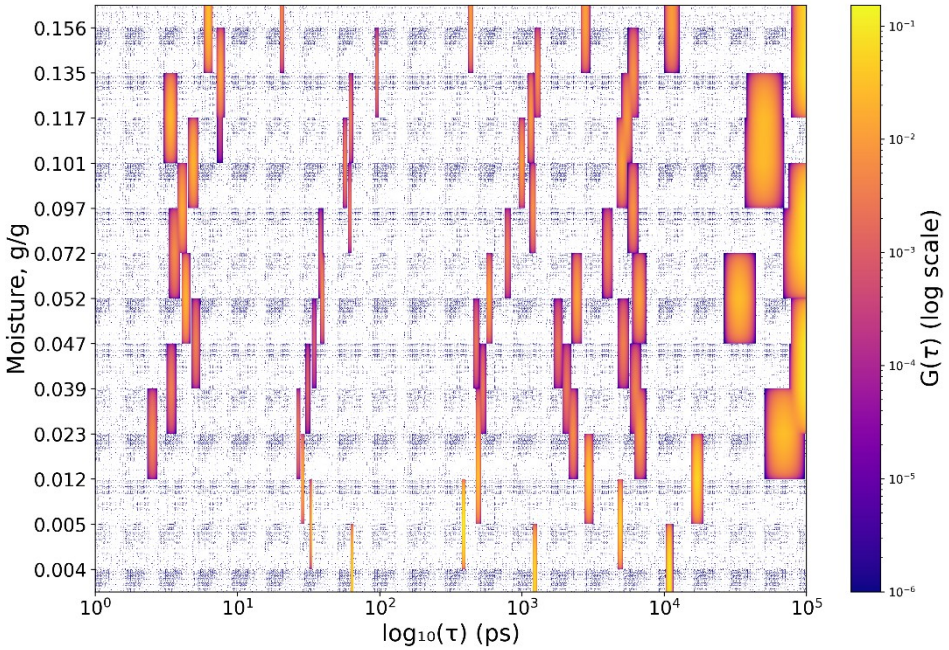


Figure 8. Diagram of RTDF variation of specimen 1 as a function of moisture.

Conclusion

As a result of the work, the CDP spectra of organo-mineral soils with different clay and organic matter contents were measured at a temperature of 25 °C, in the frequency range from 15 MHz to 15 GHz, and in the moisture range from dry state to the minimum water-holding capacity. From the obtained spectra, the RTDFs were reconstructed, and the LFLDP, HFLDP and the DC conductivity were determined.

For all studied samples, up to nine relaxations were found, which can be grouped into four groups by the closeness of τ values: 6-50 ps, 20-120 ps, 8·102 – 2·104 ps and form 104 to greater than 105 ps. Comparison with literature data allowed attributing the fourth group of relaxations to the MW relaxation, the second and third groups to bound water relaxations. The wide spread of relaxations in the second and third groups indicates a large heterogeneity of the interaction forces of bound water molecules with the surfaces of mineral and organic particles. The first group apparently includes contributions from both unbound and bound water; their separation with the using RTDF method, as in the work [16], is not possible. Nevertheless, the presence of different water categories manifests itself in the breaks of the moisture dependences of LFLDP, HFLDP and conductivity. A common trend for all samples is an increase in

relaxation times with increasing moisture, as well as an expansion of the range of τ values within each group, with the widest variability observed in the third group.

It was shown that the content of clay and organic matter have the same effect on relaxation times. At the same time, the times of the extreme high-frequency (dipole orientation relaxation) and low-frequency relaxations (MW relaxation) are practically independent of soil composition. For the relaxation with a time of about 20 ps, with increasing organic matter and clay content, an initial decrease in τ is observed when moving from specimen 1 to specimen 2, followed by an increase in specimen 3. For the relaxation with τ about 103 ps, a weak increase followed by a decrease is observed. The times of the remaining relaxations decrease.

Based on the study of three soils, a qualitative analysis of the effect of organo-mineral composition on soil properties was made. However, a detailed study of the patterns of RTDF parameters as a function of organo-mineral composition requires further studies on a larger set of soils. Nevertheless, based on the results of this work, as well as previous works [16; 17], the promise of studying soil dielectric relaxations using the RTDF reconstruction method is evident. Importantly, this method is free from a priori assumptions about the number and type of relaxators, which are inevitable when using traditional phenomenological models. The use of this method is also possible for studying dielectric relaxations in other disperse systems, such as snow cover, ice, oil-saturated reservoirs, and plant tissues (leaves, wood). Thus, the transition from phenomenological models with a fixed number of relaxations to the analysis of continuous RTDF opens new possibilities for fundamental dielectric spectroscopy of soils and creates a basis for the development of high-precision algorithmsfor radio-physical remote sensing of the Earth.

Financing: The work was carried out within the framework of the scientific topic of the State Assignment of the Kirensky Institute of Physics of the Siberian Branch of the Russian Academy of Sciences.

References

1. Dobson M.C., Ulaby F.T., Hallikainen M.T., El-Rayes M.A. Microwave dielectric behavior of wet soil-Part II: Dielectric mixing models. IEEE Transactions on Geoscience and Remote Sensing, 2007, no. 1, pp. 35-46.
2. Long D., Ulaby F. Microwave radar and radiometric remote sensing. – Artech, 2015.
3. Mironov V.L., De Roo R.D., Savin I.V. Temperature-Dependable Microwave Dielectric Model for an Arctic Soil // IEEE Transactions on Geoscience and Remote Sensing. – 2010. – Vol. 48, no. 6. – P. 2544–2556. https://doi.org/10.1109/TGRS.2010.2040034
4. Schmugge T.J. Effect of texture on microwave emission from soils // IEEE Transactions on Geoscience and Remote Sensing. – 1980. – no. 4. – P. 353–361.
5. Budzeń M. et al. Effect of soil compaction on the measurements of complex dielectric permittivity spectrum with an open-ended antenna probe and the coaxial cell system // Measurement. – 2024. – Vol. 237. – P. 115307.
6. Szypłowska A. et al. Influence of temperature on soil dielectric spectra in the 20 MHz–3 GHz frequency range // IEEE Transactions on Geoscience and Remote Sensing. – 2023. – Vol. 61. – P. 1-10.
7. Wagner N. et al. Experimental investigations on the frequency-and temperature-dependent dielectric material properties of soil // IEEE Transactions on Geoscience and Remote Sensing. – 2011. – Vol. 49. – no. 7. – P. 2518-2530.
8. Kaatze U. Complex permittivity of water as a function of frequency and temperature // Journal of Chemical and Engineering Data. – 1989. – Vol. 34, no. 4. – P. 371–374.
9. Hilhorst M.A. et al. Dielectric relaxation of bound water versus soil matric pressure // Soil Science Society of America Journal. – 2001. – Vol. 65. – no. 2. – P. 311-314.
10. Hoekstra P., Delaney A. Dielectric properties of soils at UHF and microwave frequencies // Journal of geophysical research. – 1974. – Vol. 79, no. 11. –P. 1699–1708.

11. Cole K.S., Cole R.H. Dispersion and absorption in dielectrics I. Alternating current characteristics // The Journal of chemical physics. – 1941. – Vol. 9, no. 4. – P. 341–351.
12. Macutkevic J., Banys J., Matulis A. Determination of the distribution of the relaxation times from dielectric spectra // Nonlinear analysis: modelling and control. – 2004. – Vol. 9, no. 1. – P. 75–88.
13. Tikhonov A.N., Arsenin V.Y. Solutions of ill-posed problems. – Washington: Winston & Sons, 1977. – 258 p.
14. Böttcher C.J. F., Bordewijk P. Theory of electric polarization: Volume 2. – Amsterdam: Elsevier, 1978. – 564 p.
15. Schichlein H. et al. Deconvolution of electrochemical impedance spectra for the identification of electrode reaction mechanisms in solid oxide fuel cells // Journal of Applied Electrochemistry. – 2002. – Vol. 32. – no. 8. – P. 875-882.
16. Karavayskiy A.Yu., Lukin Yu.I. The dielectric relaxation time distribution function in frozen and thawed organomineral soil over the frequency range from 10 MHz to 15 GHz // Journal of Radio Electronics. – 2026. – №. 3. https://doi.org/10.30898/1684-1719.2026.3.6 (In Russian)
17. Karavayskiy A.Yu., Lukin Yu.I. The dielectric relaxation time distribution function in frozen and thawed organomineral soil over the frequency range from 10 MHz to 15 GHz // Journal of Radio Electronics. – 2026. – №. 3. https://doi.org/10.30898/1684-1719.2026.3.6 (In Russian)
18. Mironov V.L. et al. Method of retrieving permittivity from S 12 element of the waveguide scattering matrix // 2013 International Siberian Conference on Control and Communications (SIBCON). – IEEE, 2013. – P. 1-3.
19. Loewer M. et al. Ultra-broad-band electrical spectroscopy of soils and sediments–A combined permittivity and conductivity model // Geophysical Journal International. – 2017. – Vol. 210. – no. 3. – P. 1360-1373.
20. Hasted J.B., Cole R.H. Aqueous dielectrics. – American Institute of Physics, 1975.

21. Mironov V.L. et al. Joint studies of water phase transitions in Na-bentonite clay by calorimetric and dielectric methods // Cold Regions Science and Technology. – 2018. – Vol. 153. – P. 172-180.
22. Wu A., Sun Y. Granular dynamic theory and its applications. – Springer, 2008.

For citation:

Lukin Yu.I., Karavayskiy A.Yu. The effect of clay and organic matter content on the relaxation time distribution in mineral-organic soils // Journal of Radio Electronics. – 2026. – №. 9. https://doi.org/10.30898/1684-1719.2026.9.6